Rotationally inelastic collisions of Li2(A 1Σ+ u) with Ne: Fully a b i n i t i o cross sections and comparison with experiment

Millard H. Alexander and HansJoachim Werner

Citation: The Journal of Chemical Physics **95**, 6524 (1991); doi: 10.1063/1.461522
View online: http://dx.doi.org/10.1063/1.461522
View Table of Contents: http://scitation.aip.org/content/aip/journal/jcp/95/9?ver=pdfcov
Published by the AIP Publishing

Rotationally inelastic collisions of $Li_2(A\ ^1\Sigma_u^+)$ with Ne: Fully *ab initio* cross sections and comparison with experiment

Millard H. Alexander
Department of Chemistry, University of Maryland, College Park, Maryland 20742
Hans-Joachim Werner
Fakultät für Chemie, Universität Bielefeld, D 4800 Bielefeld 1, Germany

(Received 2 May 1991; accepted 27 June 1991)

The potential energy surface (PES) for the interaction of $Li_2(A\ ^1\Sigma_u^+)$ with Ne has been computed using highly correlated multiconfiguration–reference configuration expansions (MRCI) and a large basis set. From the calculated points an analytical fit of the potential was obtained. Particular care was used to ensure a smooth fit to the angular dependence of this highly anisotropic potential. This PES has been used in exact close-coupling (CC) quantum scattering calculations of cross sections for rotationally inelastic collisions. The dependence of the calculated cross sections on velocity, as well as on the initial and final states, is found to be in excellent agreement with the measurements of Smith, Scott, and Pritchard [J. Chem. Phys. **80**, 4841 (1984);**81**, 1229 (1984)]. For comparison, cross sections were also computed within the coupled-states (CS) approximation. At low collision energies the CS results deviate significantly from both the exact CC results and the experimental data.

I. INTRODUCTION

Ever since the pioneering experiments of Bergmann and Demtröder,[1] experimental studies,[2–10] primarily in the research groups of Pritchard[2–5] and McCaffery,[6–9] of rotationally inelastic processes involving electronically excited alkali dimer molecules have provided much impetus toward the understanding of the parameters which control the efficiency of rotational energy transfer. This considerable body of experimental work has provoked a number of theoretical studies aimed at the development of simple scaling laws for rotationally inelastic collisions.[3,5,11–13] Although much of this work has involved thermal rate constants, the use of subdoppler excitation and detection schemes has allowed the determination of the actual velocity dependence of the underlying inelastic cross sections.[4,8,9,14–16] Complementary theoretical work has been limited by the difficulty of obtaining accurate potential energy surfaces (PES) for the interaction of electronically excited Li_2 or Na_2 with a noble gas partner. We have reported[17] a study of collisions of $Li_2(B\ ^1\Pi_u)$ with He and Ne, based on an early model PES developed by Poppe.[18] There have recently appeared interpolated PES for the $Li_2(A\ ^1\Sigma_u^+)$ + Ne (Ref. 19) and $Li_2(A\ ^1\Sigma_u^+)$ + He (Ref. 20) systems based on *ab initio* calculations for collinear ($C_{\infty v}$) and perpendicular (C_{2v}) geometries. In the former case, the interpolated PES was used in a semiclassical study of multipole cross sections.[19] Considerable recent theoretical attention has also been focussed on rovibrationally inelastic collisions of $Li_2(A\ ^1\Sigma_u^+)$ with Ne.[21–24] Of particular interest are the dramatic near resonant effects seen experimentally by Magill *et al.*[21,25]

In the present paper we report the results of a multireference configuration–interaction determination of the PES for the $Li_2(A\ ^1\Sigma_u^+)$ + Ne system. Calculations were performed for different values of the distance R from the center of mass of the molecule to the atom, the Li_2 bond distance r, and the angle θ between the vectors **R** and **r**. Because of the extreme anisotropy of the potential, care is required in obtaining a smooth expansion in Legendre polynomials, which is a prerequisite to a quantum scattering calculation.[26] Subsequent scattering calculations, both exact close-coupling (CC)[26] as well as within the coupled-states (CS) approximation,[27,28] were then carried out for collisions of $Li_2(A,v=9)$ + Ne at energies ranging up to 900 cm^{-1} (0.111 eV). At higher collision energies (up to 1500 cm^{-1}) only the CS approximation, which is computationally less demanding, was employed. The calculated cross sections can be compared to the results of the experiments of Smith, Scott, and Pritchard,[4] in which tuning of the excitation laser through the Doppler profile of the absorption line was used to extract the velocity dependence of the rotationally inelastic cross sections. In addition, integration over a Maxwell–Boltzmann velocity distribution can be used to determine the dependence of rotationally inelastic rate constants on the rotational quantum number of the final state. These can be compared with the experimental rate constants reported by Scott, Smith, and Pritchard.[5]

The organization of the present paper is as follows: In Sec. II we describe the *ab initio* calculations used to determine the $Li_2(A\ ^1\Sigma_u^+)$ + Ne PES. The subsequent fitting is described in Sec. III. Section IV summarizes the scattering calculations. The calculated inelastic cross sections are discussed and compared with available experimental data in Sec. V. The comparison between the CC and CS cross sections is contained in Sec. VI. The determination of the rotationally inelastic rate constants and the comparison with experiment is summarized in Sec. VII. A brief conclusion follows.

II. DESCRIPTION OF THE *Ab initio* CALCULATIONS

All electronic structure calculations reported in this paper were performed with the MOLPRO package of *ab initio* programs.[29] As is well known, the long-range dispersion

 0021-9606/91/216524-12$03.00

forces are very slowly convergent with respect to both the one-electron and N-electron basis sets. To render tractable the computational effort to compute a global, three-dimensional, potential energy surface, we had to make a compromise between accuracy and basis set size. The one-electron basis sets for Ne and Li_2 were therefore carefully optimized to reproduce as accurately as possible the known dipole polarizabilities of the fragments. The 12 s basis for Li was essentially the same as used in the accurate calculations on Li_2 by Müller and Meyer,[30] but only 6 p and 1 d (all 5 components) were included. The basis set for Ne was derived from a set optimized by Werner and Meyer[31] for the dipole polarizability. The complete basis set, which comprised 104 contracted Gaussian orbitals, is given in Table I. Some spectroscopic constants for the Li_2 molecule calculated with this basis set and 2-electron full-CI wave functions are compared to experimental data[32] and more accurate previous calculations[33,34] in Table II. The equilibrium distance obtained is slightly too long, while the harmonic frequency is 3.5 cm^{-1} too low. These small errors are due partly to basis set deficiencies and partly to the neglect of core-valence correlation.[30]

The $Li_2(A\ ^1\Sigma_u^+)$ state considered in this paper differs from the electronic ground state ($X\ ^1\Sigma_g^+$) by excitation of one electron from the $2\sigma_g$ bonding orbital into the $2\sigma_u$ antibonding orbital. This leads to a significant elongation of the molecular bond, and, as shown below, to an extremely large anisotropy in the $Li_2(A)$–Ne potential. In the presence of the perturbing Ne atom, the $D_{\infty h}$ symmetry is reduced to C_s symmetry and the states which correlate asymptotically with the $X\ ^1\Sigma_g^+$ and $A\ ^1\Sigma_u^+$ states of Li_2 both have A' symmetry. Therefore, a multiconfiguration self-consistent field (MCSCF) treatment[35–37] is necessary for a zeroth-order description of the excited state. A simple complete active space self-consistent field (CASSCF) wave function[36] with 2 electrons distributed in the $2\sigma_g$ and $2\sigma_u$ orbitals was found to be unstable with respect to small perturbations of the $D_{\infty h}$ symmetry. In order to avoid this instability, both the Li $2s$ and $2p$ orbitals have to be included in the active space, yielding a total of 8 active orbitals for the Li_2 molecule. In a natural orbital description only 8 of the 24 possible configurations contribute to the wave function, since only 2 electrons are correlated. For the $Li_2(A)$ + Ne calculations the direct product of this MCSCF wave function for Li_2 and the SCF wave function for Ne was used as the reference space in subsequent internally contracted MRCI calculations.[38,39] At each geometry the average energy of the X and A states was optimized in the MCSCF procedure. In order to avoid undesired MCSCF solutions in which some of the excited Li_2 orbitals are replaced by excited Ne orbitals, the correct asymptotic solution was used as a starting guess in the orbital optimizations. The internally contracted MRCI calculations[38,39] included all single and double excitations from the reference wave function into all active and virtual orbitals.

The interaction energies were computed using the counterpoise method,[40] i.e., at each geometry the fragment energies were calculated with the basis functions of the other fragment present and then subtracted from the energy of the total system. Since the wave function is not size consistent, the asymptotic energy of the total system is not equal to the sum of the individually calculated fragment energies, and the interaction energy obtained by the counterpoise method is not zero at large distances. It was assumed that this size consistency error is independent of R and θ and subtracted from the interaction energies at all geometries. Hence, the interaction potential $V(R,r,\theta)$ was obtained as

$$V(R,r,\theta) = E_{Li_2-Ne}(R,r,\theta) - E_{Li_2}(R,r,\theta) - E_{Ne}(R,R,\theta) - \Delta E(\infty,r) \quad (1)$$

with

$$\Delta E(\infty,r) = E_{Li_2-Ne}(R=\infty,r) - E_{Li_2}(R=\infty,r) - E_{Ne}(R=\infty). \quad (2)$$

Depending on the Li_2 bond distance r, the size consistency correction $\Delta E(\infty,r)$ varied between 111 and 124 cm^{-1}. In total, interaction energies were computed for more than 300 geometries.

III. FITTING THE *Ab initio* POINTS

In the standard quantum treatment[26] of inelastic scattering between a molecule in a $^1\Sigma$ electronic state and a structureless atom, the atom–molecule interaction potential, which is a function of the molecular bond length r, the distance R between the atom and the center of mass of the molecule, and the angle θ between $\mathbf{r}$ and $\mathbf{R}$, is expanded in Legendre polynomials in the angle θ, namely,

TABLE I. GTO basis set used in the *ab initio* calculations.[a]

Li:	s	3914.1032(0.000 291), 479.038 46 (0.002 250), 108.556 41 (0.011 773), 30.271 67 (0.047 954), 9.660 83 (0.148 356), 3.392 72, 1.275 24, 0.497 59, 0.096 96, 0.049 76, 0.022 85, 0.011 00
	p	2.0 (0.008 314), 0.5 (0.035 469), 0.11, 0.05, 0.02, 0.009
	d	0.091
Ne:	s	49 014.207 (0.000 208), 7373.0472 (0.001 63), 1653.1857 (0.008 641), 460.984 66 (0.036 130), 145.723 68 (0.122 508), 50.368 73, 18.804 44, 7.460 14, 2.098 42, 0.784 82, 0.294 67, 0.1
	p	130.050 14 (0.004 230), 30.575 74 (0.030 413), 9.651 66 (0.118 913), 3.560 28, 1.413 67, 0.572 60, 0.24, 0.1
	d	2.2, 0.7, 0.2
	f	0.44

[a] All exponents in $bohr^{-2}$. Contraction coefficients in parentheses.

TABLE II. Calculated spectroscopic constants for Li_2.[a]

State	R_e	ω_e	$\omega_e x_e$	α_e
$X\ ^1\Sigma_g^+$	2.713[b]	343.0	2.51	0.0066
	2.669[c]	351.7	2.47	0.0071
Expt.[c]	2.673	351.4	2.61	0.0070
$A\ ^1\Sigma_u^+$	3.154[b]	252.0	1.54	0.0052
	3.108[d]	256.1	1.60	0.0055
Expt.[e]	3.108	255.5	1.58	0.0054

[a] R_e in Ångstroms, other values in cm^{-1}.
[b] This work.
[c] Reference 30.
[d] Reference 34.
[e] Reference 32 and references contained therein.

$$V(r,R,\theta) = \sum_{\lambda=0}^{N} V_\lambda(r,R) P_\lambda(\cos\theta). \tag{3}$$

In the case of collisions of a homonuclear diatomic (as is the situation under study here), the symmetry of the potential to interchange of the nuclei restricts this expansion to even-order Legendre polynomials. Because of the extreme anisotropy of the $Li_2(A)$ + Ne PES, it was difficult to obtain a smooth expansion. The fitting procedure used is outlined below.

From a grid of *ab initio* points $V(r_i,R_j,\theta_k)$ the usual procedure is to obtain the expansion coefficients in Eq (3) for each (r_i,R_j) pair by a least-squares fit of as many angular points as are available ($\theta_k, k = 1,...,n$) in terms of the n lowest-order Legendre polynomials. In the present case this procedure was unsatisfactory for the following reasons: The elongation of the Li_2 molecule implies that for collinear approach the Ne atom is strongly repelled even at rather large distances, but can approach quite closely at perpendicular geometries. Understandably, this anisotropy becomes more pronounced as the Li_2 bond distance r increases. For moderate values of R, the interaction energy was found to vary by up to 2 orders of magnitude as the angle θ ranged from 0° to 90°. For most pairs of the coordinates (r_i,R_j) *ab initio* MRCI points were calculated at 5 or 6 angles. Because of the extreme variation in the interaction potential, attempts at a direct fit in terms of the lowest 5 or 6 Legendre polynomials resulted in unphysical oscillations in the potential as a function of θ. This type of behavior can be clearly seen in the fit by Cooper *et al.* of the analogous $Li_2(A\ ^1\Sigma_u^+)$ + He potential.[20] Worse, these spurious oscillations often resulted in artificial wells (negative interaction energies) for near perpendicular geometries. Similar difficulties have been reported by Schinke and co-workers[41] in the fitting of an *ab initio* potential for the interaction of Na_2 in its ground electronic state ($X\ ^1\Sigma_g^+$) with Ne.

In principle, the lack of smoothness in the Legendre fit could be eliminated by using a large number of Legendre terms in the expansion.[20,42,43] In the present case this is not possible, due to the relatively small set of angular points at which *ab initio* calculations were performed. A more indirect approach involves choosing an alternate expansion which can fit the *ab initio* data smoothly, with only a limited number of parameters. Subsequently, to carry out scattering calculations, this initial expansion can be reexpanded in terms of Legendre polynomials. The approach we developed is outlined below.

Since the form of the potential (high sharp peak at $\theta = 0°$, broad minimum at 90°) was suggestive of a $\cos^m\theta$ dependence with a large value of m, we thought that a more successful fitting procedure would involve a selection of individual powers of $\cos\theta$. The following algorithm was used to obtain accurate, smooth fits: For each (r_i,R_j) pair, the potential was expanded as

$$V(r_i,R_j,\theta) = C_{ij}^{(0)} + C_{ij}^{(2)}\cos^2\theta + \sum_{m=1}^{M} C_{ij}^{(n_m)}(\cos\theta)^{n_m}. \tag{4}$$

Typically only two (and never more than three) terms were taken in the sum ($M = 2,3$). The coefficients were obtained by a least-squares fit to however many *ab initio* interaction energies were available at different angles for a given (r_i,R_j) pair. Points with interaction energies greater than 0.5 hartree, which correspond to regions of the potential surface which are totally inaccessible in the experiments of Smith and co-workers,[4] were not included in the fit. In the least-squares fits the points were weighted inversely proportional to their energy. The powers n_m included in the expansion were limited to the range $4 \leqslant n_i \leqslant n_{i+1} \leqslant \cdots \leqslant n_M \leqslant 18$. The individual values were initially chosen as low as possible ($n_1 = 4$, $n_2 = 6,...,n_M = 2M + 2$), and then successively (first n_M, then n_{M-1}, then n_{M-2}, and so on) increased until the resulting fit was found to satisfy the following criteria for smoothness over the range $0° \leqslant \theta \leqslant 90°$: (1) the derivative $\partial V(r_i,R_j,\theta)/\partial\theta$ was always negative; (2) there could be no more than two inflection points; and (3) if two inflection points occurred, the value of $\partial V/\partial\theta$ at the second inflection point (at larger θ) could be no larger than 1% of the value of $\partial V/\partial\theta$ at the first inflection point. An additional restriction limited the largest power n_M used at each Li_2–Ne distance R_i to be no larger than the largest power used at the nearest smaller distance, R_{i-1}. As might have been anticipated, large values of the powers n_m were required only at relatively small values of R. For $R \geqslant 10$, where the extreme anisotropy of the potential is less apparent, accurate fits could be obtained using just the lowest powers ($n_m = 4,6,8$).

Once the expansion coefficients in Eq. (4) were obtained as described above, the known expansion coefficients of the Legendre polynomials in powers of $\cos\theta$ were used to reexpress the angular dependence in terms of Legendre polynomials, namely,

$$V(r_i,R_j,\theta) = \sum_{\lambda=0}^{(n_M)_i} D_{ij}^{(\lambda)} P_\lambda(\cos\theta). \tag{5}$$

Note that the highest order of the Legendre polynomials in the expansion is equal to one more than the maximum power $(n_M)_i$ used in the expansion in powers of $\cos\theta$. For each discrete value of the Li_2 internuclear distance r_i, the interaction potential was then interpolated as a continuous function of R

$$V(r_i,R,\theta) = \sum_{\lambda=0}^{(n_M)_i} f_{r_i}^{(\lambda)}(R) P_\lambda(\cos\theta), \tag{6}$$

where the sum runs up to the maximum power used at the smallest Li_2–Ne distance, R_1, in the expansion in powers of $\cos\theta$ [Eq. (4)]. The following choice was made for the interpolation polynomials: Exponential extrapolation was used for $R<R_1$. A spline interpolation of the *logarithm* of the $D_{ij}^{(\lambda)}$ coefficients, subsequently re-exponentiated, was used for $R_1 \leqslant R \leqslant R_n$, were the index n corresponds to the last *positive* value of $D_{ij}^{(\lambda)}$. If the subsequent values of the $D_{ij}^{(\lambda)}$ coefficients with $j \geqslant n$ were all zero (this was the case for $\lambda \geqslant 6$), then an exponential extrapolation was used for $R>R_n$. For $\lambda = 0,2,4$, a regular spline interpolation of the $D_{ij}^{(\lambda)}$ coefficients was used for $R_n \leqslant R \leqslant 20$ bohr, with an R^{-6} extrapolation for $R>20$ bohr.

In the description of the rotationally inelastic scattering, discussed below, appear vibrationally averaged matrix elements of the interaction potential, namely,

$$V_{v'v}(R,\theta) \equiv \int \chi_{v'}(r) V(r,R,\theta) \chi_v(r) dr, \tag{7}$$

where $\chi_v(r)$ designates the wave function for the vth vibrational level of the $A\ ^1\Sigma_u^+$ state of Li_2. To evaluate these integrals we assumed the dependence of the potential on the Li–Li distance could be expanded as a quadratic function, namely,

$$V(R,\theta) = \sum_{\lambda=0}^{n_{\max}} [v_0^{(\lambda)}(R) + v_1^{(\lambda)}(R)\cdot(r-r_0) + v_2^{(\lambda)}(R)\cdot(r-r_0)^2] P_\lambda(\cos\theta), \tag{8}$$

where $n_{\max}$ is the maximum value of n_m for the fits at the different r_i. With Eq. (8), the vibrationally averaged matrix elements can be expressed as

$$V_{v'v}(R,\theta) = \sum_{\lambda=0}^{n_{\max}} [v_0^{(\lambda)}(R) + v_1^{(\lambda)}(R)\langle v'|(r-r_0)|v\rangle + v_2^{(\lambda)}(R)\langle v'|(r-r_0)^2|v\rangle] P_\lambda(\cos\theta). \tag{9}$$

A practical difficulty in the implementation of the procedure defined by Eqs. (8) and (9) arises from the fact that the $v=9$ level of the $A\ ^1\Sigma_u^+$ state of Li_2, which was excited in the experiments of Smith *et al.*,[4] the average internuclear separation $\langle v|r|v\rangle$ is ~ 6.5 bohr, which is substantially larger than the equilibrium internuclear separation in this state ($r_e = 5.8733$ bohr, see Table II). Thus the *ab initio* calculations, which were carried out at Li_2 distances of $r_i = 5.05$, 5.8733, and 6.6 bohr, sample unevenly the range of Li–Li distances accessible to the molecule in moderately high vibrational levels ($7 \leqslant v \leqslant 11$). With this caveat, we found that the smoothest representation of the *diagonal* (in v) potential matrix elements was obtained using just the calculated points at $r = 5.8733$ and 6.6 bohr to obtain a two-term expansion with, in Eq. (9), $r_0 = 6.6$ bohr. We have, in this case,

$$v_0^{(\lambda)}(R) = f_{r=6.6}^{(\lambda)}(R), \tag{10a}$$

TABLE III. Matrix elements $\langle v'|(r-r_0)^n|v\rangle$ for the $A\ ^1\Sigma_u^+$ state of Li_2, with $r_0 = 5.8733$ bohr.[a]

v'	$v=7$	8	9	10	11
			$n=1$		
7	0.516 73				
8	0.748 22	0.588 84			
9	−0.095 47	0.795 89	0.662 01		
10	0.018 19	−0.106 98	0.841 38	0.735 53	
11	−0.004 22	0.021 33	−0.118 57	0.885 04	0.810 23
			$n=2$		
7	1.328 76				
8	0.689 62	1.559 14			
9	0.509 63	0.829 90	1.803 68		
10	−0.143 89	0.561 45	0.980 36	2.061 80	
11	0.039 44	−0.167 44	0.611 31	1.140 93	2.335 13

[a] Determined from potential curves given in Ref. 34.

$$v_1^{(\lambda)}(R) = [f_{r=6.6}^{(\lambda)}(R) - f_{r=5.8733}^{(\lambda)}(R)]/(6.6-5.8733), \tag{10b}$$

and

$$v_2^{(\lambda)}(R) = 0. \tag{10c}$$

For an accurate determination of the *off-diagonal* (in v) potential matrix elements, which are needed for the calculation of cross sections for vibrationally inelastic transitions,[24] it is necessary to include both the linear and quadratic terms in Eq. (9). In this case we use a three point fit, obtaining, with $r_0 = 5.8733$ bohr,

$$v_0^{(\lambda)}(R) = f_{r=5.8733}^{(\lambda)}(R), \tag{11a}$$

$$v_1^{(\lambda)}(R) = -0.570\,523 f_{r=5.05}^{(\lambda)}(R) - 0.159\,982 f_{r=5.8733}^{(\lambda)}(R) + 0.730\,506 f_{r=6.6}^{(\lambda)}, \tag{11b}$$

and

$$v_2^{(\lambda)}(R) = 0.785\,088 f_{r=5.05}^{(\lambda)}(R) - 1.673\,46 f_{r=5.8733}^{(\lambda)}(R) + 0.888\,369 f_{r=6.6}^{(\lambda)}. \tag{11c}$$

For $r_0 = 5.8733$ bohr, for the $v = 7$–11 levels of the $A\ ^1\Sigma_u^+$ state of Li_2 the matrix elements of $(r-r_0)$ and $(r-r_0)^2$ were determined by numerical quadrature of the $Li_2(A)$ vibrational wave functions obtained by Numerov integration of the $A\ ^1\Sigma_u^+$ state potential curves.[33,44] These matrix elements, which are tabulated in Table III, can also be used to calculate the matrix elements of $(r-r_0)$ with $r_0 = 6.6$ bohr, which is needed in the implementation of Eq. (10).

As an example, Fig. 1 shows a contour plot of the $\langle v=9|V|v=9\rangle$ interaction potential as a function of the orientation of the Ne atom with respect to the Li_2 molecule.[45] The extreme anisotropy of the potential is clearly apparent; rather than a rigid ellipsoid the PES resembles an inverted bathtub. Also surprising is the extremely small size

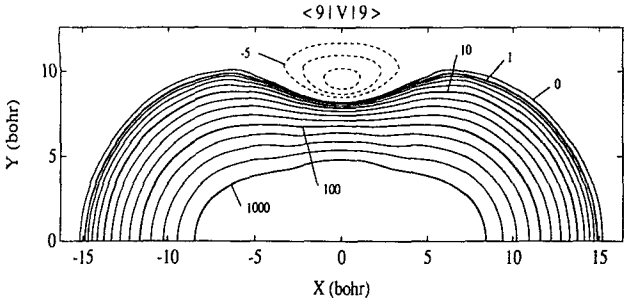

FIG. 1. Contour plot of the diagonal $\langle v=9|V|v'=9\rangle$ vibrationally averaged $Li_2(A\ ^1\Sigma_u^+)$–Ne interaction potential in cm^{-1}. The Li_2 molecule lies along the X axis. At the equilibrium internuclear separation in the $v=9$ level, the two Li atoms lie at ± 3.25 bohr. The dashed lines indicate negative contours at $E=-5$, -7, and $-9\ cm^{-1}$. The contours between 1 and 1000 cm^{-1} are equally spaced on a logarithmic scale. The figure is presented so that the distance scale is identical for both the X and Y axis.

of the attractive well, which is less than 15 cm^{-1} deep. It should be noted, however, that the true potential might be significantly deeper, since it is likely that the orbital and configuration basis sets used in the *ab initio* calculations are not fully converged with respect to the long-range dispersion energy. Figure 2 illustrates the dependence on R of the vibrationally averaged $V_{vv}(R,\theta)$ potential for $v=9$, for several different values of the angle. We observe that the dependence on R is quite complex, and in the short-range region could not be well approximated by a simple exponential or power law repulsion. The structure in the repulsive wall of the potential seen in the upper panel of Fig. 2 likely reflects the fact that at moderate distances the dominant repulsive interaction is between the Ne atom and the relatively diffuse Li_2 $2p_\sigma$ orbital. As the Ne atom penetrates to shorter range, it begins to feel a sharply stronger repulsive interaction with the much more dense electronic core. Analogous structure in the repulsive region of the potential energy surfaces for the interaction of Na_2 in the ground $(X\ ^1\Sigma_g^+)$ electronic state with He and Ne has been reported by Häusler, Schinke, and co-workers.[41,46]

In a similar manner Fig. 3 illustrates the dependence on θ of the same potential, for several different values of the Li_2–Ne separation R. The marked anisotropy of the potential is seen clearly here: For perpendicular approach at thermal energies (100–600 cm^{-1}), the Ne atom can penetrate to within ~ 6.5 bohr, while for collinear approach, the classical turning point lies ~ 3 bohr further out.

Finally, Fig. 4 illustrates the dependence on the Li_2 bond distance r of the potential, as given by Eqs. (9) and (11), at several values of the Li_2–Ne separation R for both collinear and perpendicular approach of the Ne atom. We observe that the derivative of the potential with respect to r is much larger for collinear geometries. This implies that vibrationally inelastic transitions, which are induced by this derivative, will be induced preferentially by collisions in which the Li_2 and Ne encounter one another in collinear geometry. We also observe that contrary to what one might expect, for perpendicular collisions at moderate to long range, the approach of the Ne atom induces a *contraction* of the Li_2 bond. Eventually, at shorter range the Ne atom burrows into the Li_2 molecule and forces the bond apart. This effect has been noted earlier in a study of the similarly repulsive H_2–He system.[47]

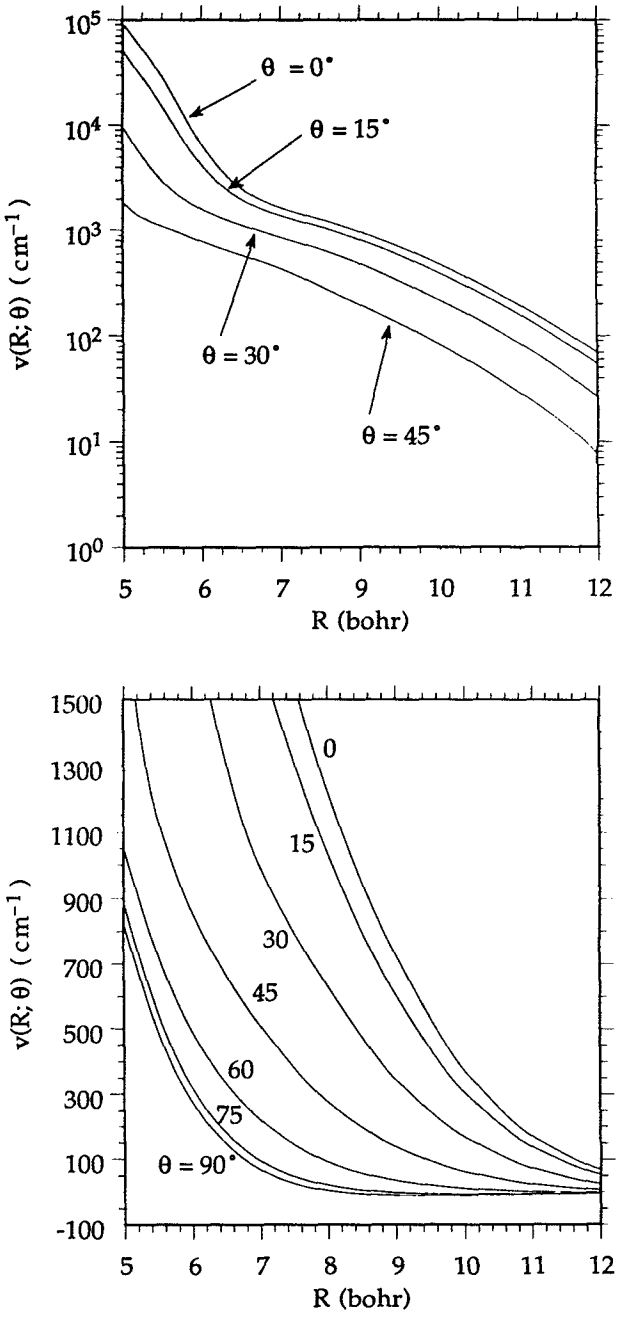

FIG. 2. Plot of the vibrationally averaged $Li_2(A\ ^1\Sigma_u^+)$–Ne interaction potential $V_{vv}(R,\theta)$ for $v=9$ in cm^{-1} as a function of the Li_2–Ne distance for several different values of θ. The upper and lower panels are designed to illustrate the behavior of the potential in the extreme repulsive region as well as at long range.

IV. SCATTERING CALCULATIONS

The quantum close-coupled (CC) treatment of rotationally inelastic collisions of a molecule in a $^1\Sigma$ electronic state with a spherical target, due originally to Arthurs and Dalgarno,[26] is well documented[48,49] and will consequently

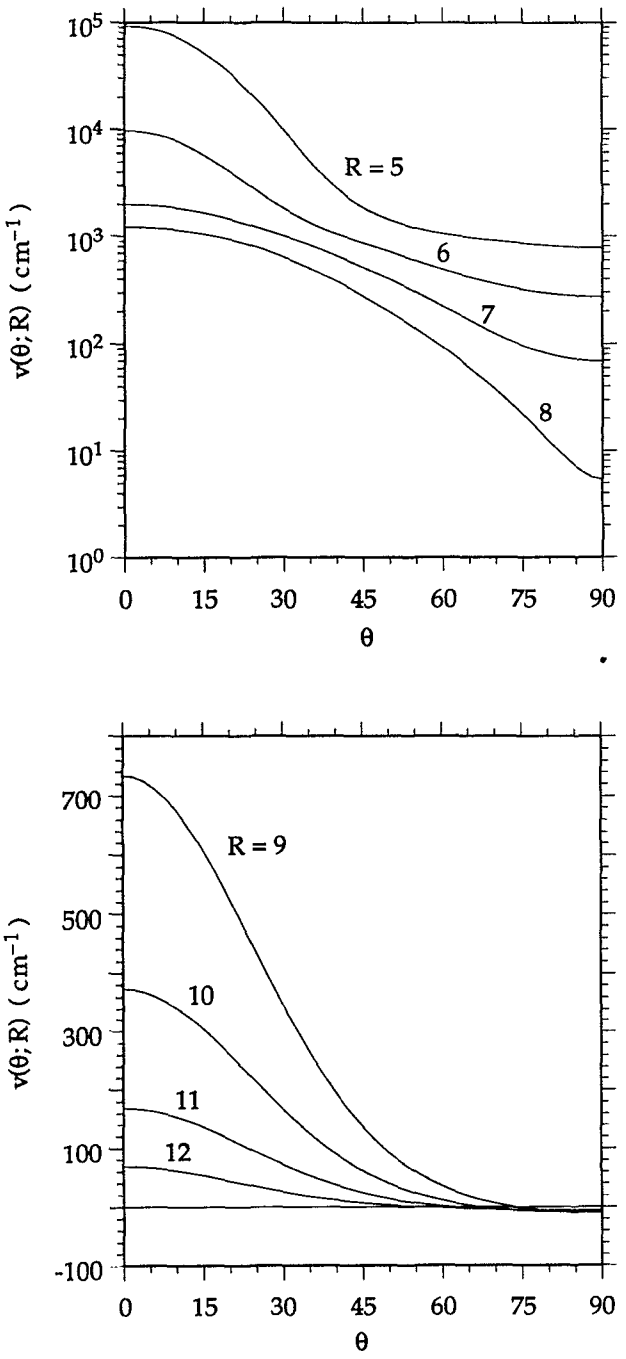

FIG. 3. Plot of the vibrationally averaged $Li_2(A\ ^1\Sigma_u^+)$–Ne interaction potential $V_{v0}(R,\theta)$ for $v = 9$ in cm^{-1} as a function of the LiLiNe angle for several different values of R. The upper and lower panels are designed to illustrate the behavior of the potential in the extreme repulsive region as well as at long range.

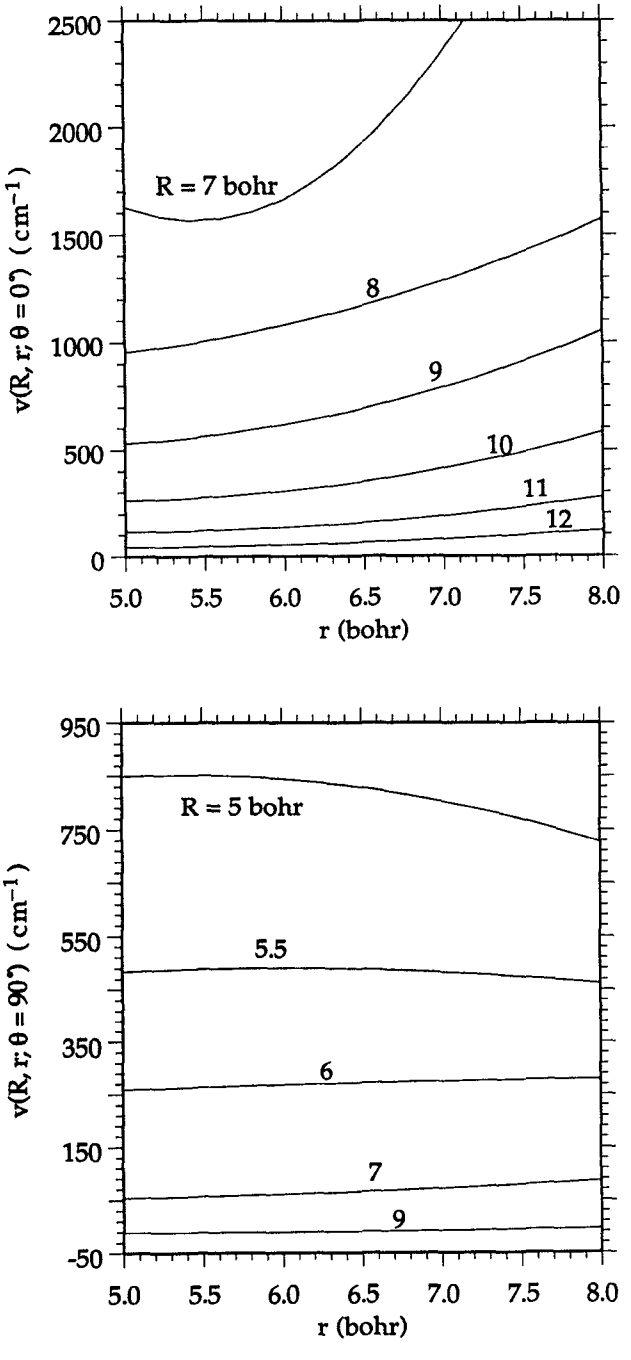

FIG. 4. Plot of the dependence of the $Li_2(A\ ^1\Sigma_u^+)$–Ne interaction potential $V(R,r,\theta)$ in cm^{-1} as a function of the LiLi distance for several different values of R, as given by Eqs. (9) and (10). The upper and lower panels illustrate the behavior of the potential for, respectively, collinear and perpendicular LiLiNe geometries.

not be reviewed in detail. The total scattering wave function is expanded in terms of a product of rotational wave functions of the Li_2 molecule multiplied by wave functions describing the orbital motion of the Li_2–Ne pair. The coefficients in this expansion satisfy the usual CC equations.[26,48,49] The asymptotic behavior of these solutions define the scattering S matrix, from which one can extract inelastic transition probabilities. Inelastic cross sections are obtained as a weighted sum of these transition probabilities, which extends over all values of the total angular momentum for which the transition probabilities are non-negligible. In the expansion of the scattering wave function one must include enough internal molecular rotational levels so that the probability for the transition from an initial rotational level j to a final level j' is converged with respect to increasing the size of the basis. The major practical difficulty is that the number of

terms in this expansion scales roughly as j_{max}^2, where j_{max} is the maximum rotational quantum number included in this expansion,[50] while the numerical effort required in solution of the CC equations scales as N^3, where N is the total number of terms (channels) included in the expansion.[51] Thus the overall numerical effort sales as j_{max}^6.

By decoupling the rotational and orbital angular momenta, as is accomplished in the coupled-states (CS) approximation,[27,28] the numerical effort can be reduced to roughly $2j_{max}^4$. For collisions involving a basically repulsive interaction, as is certainly the case for $Li_2(A)$ + Ne where the well depth is only $\sim 15\ cm^{-1}$, previous work[52–54] suggests that the CS method should be quite accurate.

We have carried out both CC and CS determinations of cross sections for the collision of $Li_2(A\ ^1\Sigma_u^+)$ with Ne, using the potential energy surface described in Sec. III. The rotational constants and potential matrix elements [Eqs. (7)–(10)] appropriate to the $v = 9$ level of the A state were used,[32] since it is this level which was excited in the experiments of Smith *et al.*[4] The Hibridon scattering package[55] was used to solve the CC and CS equations. Calculations were carried out at total energies ranging up to $900\ cm^{-1}$ (in the case of the CC calculations) and up to $1700\ cm^{-1}$ (in the case of the CS calculations). To obtain convergence it was necessary to include in the channel basis all energetically accessible (open) rotational levels as well as at least the lowest energetically inaccessible (closed) level. At lower energies, two energetically closed levels were included. For the CC calculations at the highest energy ($900\ cm^{-1}$) this implied a total of 529 channels.

V. CALCULATED CROSS SECTIONS AND COMPARISON WITH EXPERIMENT

Figures 5–8 display representative CC cross sections for transitions out of the $J = 8$ and $J = 22$ rotational levels of the $v = 9$ manifold of the A state of Li_2 as a function of the initial relative collision velocity.[56] The transitions featured were those for which a direct comparison could be made with the experimentally determined cross sections of Smith *et al.*[4] The agreement between theory and experiment is in general excellent, virtually within the experimental error bars, particularly at higher energy. The cross sections, both for upward transitions, which have thresholds imposed by the exoergicity of the transition, and for downward transitions, which are energetically accessible even at zero collision energy, show the rise and subsequent fall as a function of collision velocity commented on by Smith *et al.*[4] The drop in the inelastic cross sections at low collision velocity, denoted "rotational suppression" by Smith *et al.*,[4] is a manifestation of a well-known effect, pointed out first by Miller.[57] The "classical" threshold for a transition—the energy at which there exists at least one classically allowed trajectory connecting the classically correspondent initial and final states in question—is often higher than the energetic threshold. In a semiclassical sense transition probabilities at energies below this classical threshold correspond to trajectories which tunnel outside of the classically allowed region of phase space.

The decrease in the cross sections at higher collision velocity most likely occurs because the incoming collision flux can become distributed among an increasingly large number of final states. Smith *et al.*[4] attributed this decrease to the increasing probability of *vibrationally* inelastic transi-

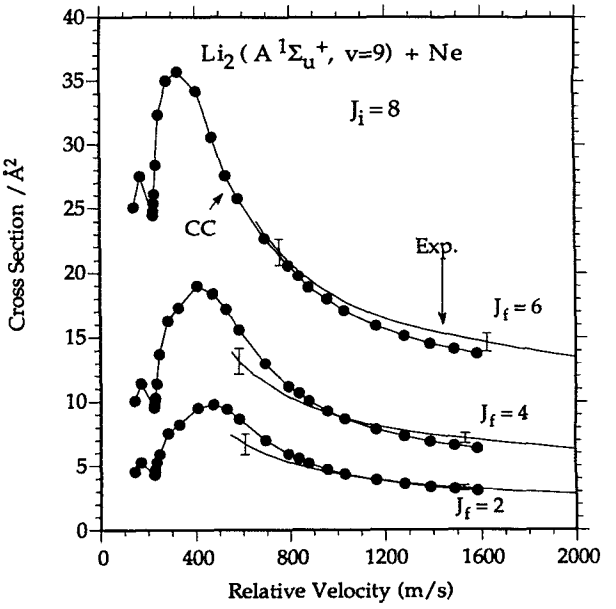

FIG. 5. Rotationally inelastic cross sections, as a function of the collision velocity, for downward ($J_{final} < J_{initial}$) transitions out of the $J = 8$ rotational level of the $v = 9$ manifold of $Li_2(A\ ^1\Sigma_u^+)$ in collisions with Ne. The filled circles denote the results of the present CC calculations and the solid curves are the results of the deconvolution of the velocity selected experimental rate constants, as described in Ref. 4. The experimental error bars are taken from Ref. 4.

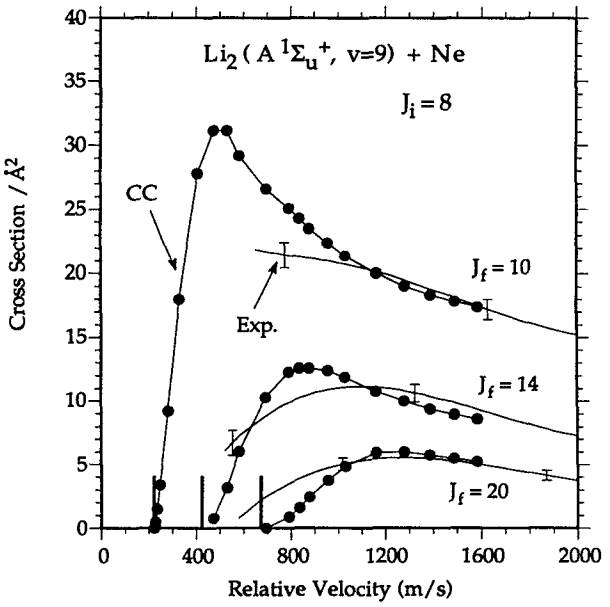

FIG. 6. Rotationally inelastic cross sections, as a function of the collision velocity, for upward ($J_{final} > J_{initial}$) transitions out of the $J = 8$ rotational level of the $v = 9$ manifold of $Li_2(A\ ^1\Sigma_u^+)$ in collisions with Ne. The filled circles denote the results of the present CC calculations and the solid curves are the results of the deconvolution of the velocity selected experimental rate constants, as described in Ref. 4. The experimental error bars are taken from Ref. 4. The energetic thresholds for the three final states (J_{final} = 10, 14, and 20) are shown as heavy vertical bars.

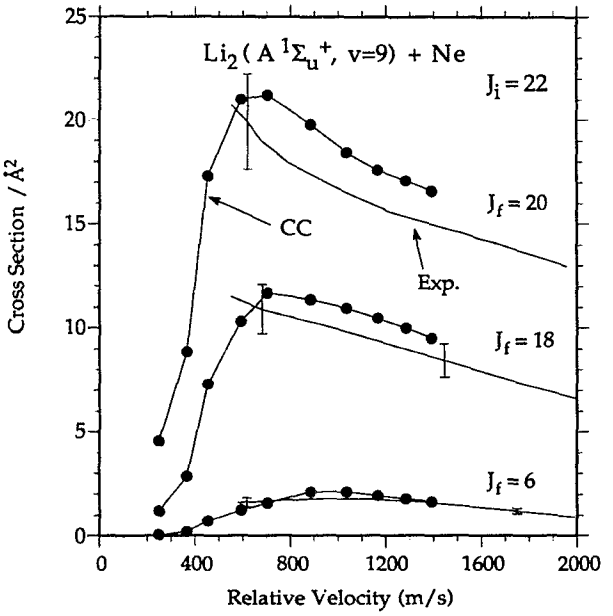

FIG. 7. Rotationally inelastic cross sections, as a function of the collision velocity, for downward ($J_{final} < J_{initial}$) transitions out of the $J = 22$ rotational level of the $v = 9$ manifold of $Li_2(A\ ^1\Sigma_u^+)$ in collisions with Ne. The filled circles denote the results of the present CC calculations and the solid curves are the results of the deconvolution of the velocity selected experimental rate constants, as described in Ref. 4. The experimental error bars are taken from Ref. 4 but include also the additional $\pm$ 10% uncertainty in the measured magnitude of the cross sections as discussed on p. 1236 of Ref. 4.

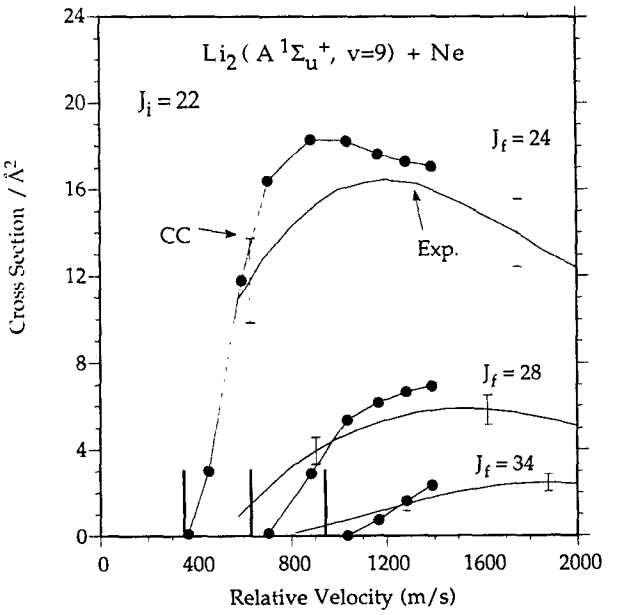

FIG. 8. Rotationally inelastic cross sections, as a function of the collision velocity, for upward ($J_{final} > J_{initial}$) transitions out of the $J = 22$ rotational level of the $v = 9$ manifold of $Li_2(A\ ^1\Sigma_u^+)$ in collisions with Ne. The filled circles denote the results of the present CC calculations and the solid curves are the results of the deconvolution of the velocity selected experimental rate constants, as described in Ref. 4. The experimental error bars are taken from Ref. 4 but include also the additional $\pm$ 10% uncertainty in the measured magnitude of the cross sections as discussed on p. 1236 of Ref. 4. The energetic thresholds for the three final states (J_{final} = 24, 28, and 34) are shown as heavy vertical bars.

tions as the relative velocity increases. However, since we did not allow vibrational inelasticity in our calculations, and since we agree so well with experiment at the higher collision velocities, we feel that the loss of flux to vibrationally inelastic transitions is likely an unimportant effect, at least for collision velocities less than 2000 m/s. This is also consistent with our preliminary calculations on vibrationally inelastic collisions of $Li_2(A)$ with Ne,[24] which showed that the cross sections for vibrationally inelastic transitions out of low rotational levels are fairly small.

We feel that the overall excellent agreement between our calculated cross sections and those determined experimentally by Smith *et al.*[4] implies that the present MRCI calculations, and the subsequent analytical fit, result in an accurate description of the $Li_2(A)$ + Ne interaction, at least over the range of energies sampled here. The largest discrepancies between our calculated cross sections and the experimental values[4] occur at low velocities. One possible explanation is that the deconvolution method used,[4,14,15] and the inescapable spread in velocities due to the significant spread in the velocity of the relatively light Ne atom, results in an imprecision in the experimentally determined cross sections which becomes increasingly significant as the collision velocity decreases. On the other hand, errors in the computed values for low collision energies could arise from inaccuracies in the long range part of the *ab initio* potential.

Figure 9 offers more insight into the near threshold dependence of several endoergic ($J = 0, 8 \rightarrow 10$) and exoergic ($J = 8 \rightarrow 6,2$) transitions as a function of the collision velocity just above threshold. Except just at threshold, the cross sections for both endoergic processes increase with a simple power-law dependence on the final state velocity above threshold. The power ranges from $\sim$2.5 for the $8 \rightarrow 10$ transition to $\sim$3.0 for the $0 \rightarrow 10$ transition. The cross sections for the exoergic $8 \rightarrow 6.2$ transitions also show a smooth decrease down to threshold, except just at the threshold for opening of the $J = 10$ final state, where a slight drop in these inelastic cross sections appears. (This can be seen in Fig. 5.) The exponent in the power law dependence on velocity is considerably flatter than for the endoergic cross sections; 0.51 in the case of the $8 \rightarrow 6$ transition and 0.64 in the case of the $8 \rightarrow 2$ transition.

VI. COMPARISON BETWEEN CLOSE-COUPLED AND COUPLED-STATES CROSS SECTIONS

Figures 10 and 11 display a comparison of CS and CC cross sections for those transitions out of the $J = 8$ level of the $v = 9$ manifold which are compared with experiment in Figs. 5 and 6. As can be seen, for both exo- and endoergic transitions the CS cross sections agree reasonably well with the exact CC values at high collision velocities. At lower velocity the degree of agreement deteriorates. Additionally, there is an overall oscillatory behavior superimposed on the velocity dependence of the CS cross sections which is not apparent in the more exact CC values.

The poor accuracy of the CS approximation is surprising, since one might expect[54,58] this approximation to be well suited to the $Li_2(A)$ + Ne system, where the molecule has a

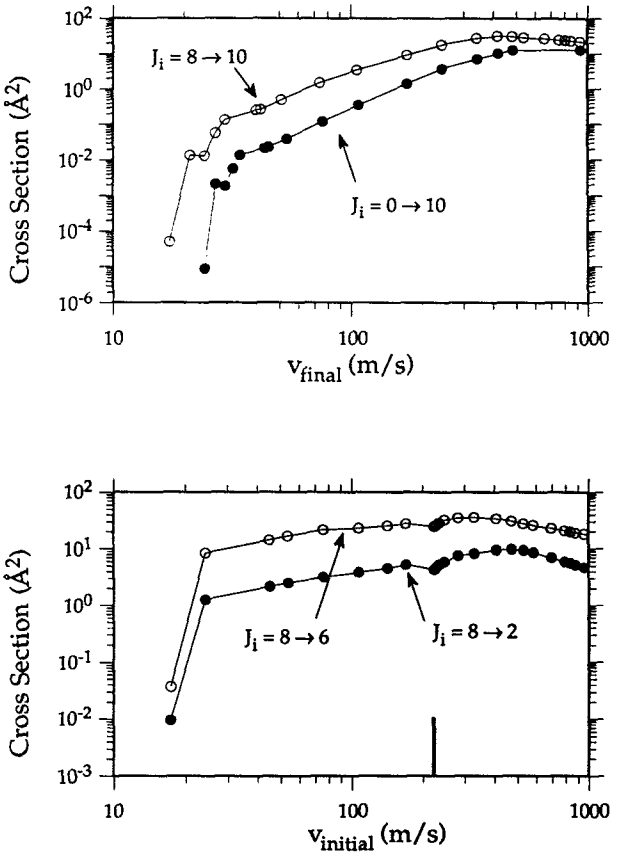

FIG. 9. (Upper panel) Rotationally inelastic CC cross sections for the $J = 0 \rightarrow J = 10$ (filled circles) and $J = 8 \rightarrow J = 10$ (open circles) transitions in the $v = 9$ manifold of $Li_2(A\ ^1\Sigma_u^+)$ in collision with Ne. These are plotted as a function of the collision velocity above the threshold for formation of the $J = 10$ state. (Lower panel) Rotationally inelastic CC cross sections for the $J = 8 \rightarrow J = 2$ (filled circles) and $J = 8 \rightarrow J = 6$ (open circles) transitions in the $v = 9$ manifold of $Li_2(A\ ^1\Sigma_u^+)$ in collisions with Ne plotted as a function of the collision velocity in the initial ($J = 8$) level. The threshold for appearance of the $J = 10$ final state is indicated by the vertical heavy bar.

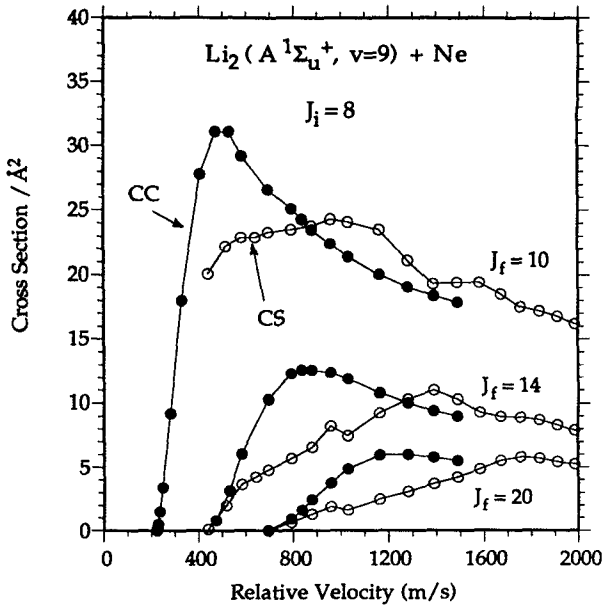

FIG. 10. Rotationally inelastic cross sections, as a function of the collision velocity, for upward ($J_{final} > J_{initial}$) transitions out of the $J = 8$ rotational level of the $v = 9$ manifold of $Li_2(A\ ^1\Sigma_u^+)$ in collisions with Ne. The filled circles denote the results of the present CC calculations while the open circles indicate the results of calculations done within the coupled-states (CS) approximation.

small rotational constant ($B = 0.45\ cm^{-1}$) and the potential is dominantly repulsive, with a negligibly small attractive well. Early tests of the accuracy of the CS approximation[54] involved systems in which the anisotropy of the potential was much less pronounced than in the present case. Recently, Werner and co-workers have found the CS approximation to be quite accurate for collisions of $OH(A\ ^2\Sigma^+)$ with Ar (Ref. 53) and He (Ref. 52). The anisotropy of these potentials is quite pronounced, especially in the former case. However, comparisons have been reported for collisions of Ar with CH_4 (Ref. 59) and with H_2O (Ref. 60) in which the relative error in the CS cross sections has been as large as 30–40 %, comparable to that seen here.

VII. THERMAL RATE CONSTANTS FOR ROTATIONAL ENERGY TRANSFER

Scott, Smith, and Pritchard[5] also measured thermal rate constants for the rotational relaxation of $Li_2(A\ ^1\Sigma_u^+)$ in collisions with Ne. For a particular $j \rightarrow j'$ transition, the thermal rate constant is defined by[61]

$$k_{J \rightarrow J'}(T) = N(T) \int v^3 \sigma_{J \rightarrow J'}(v) \times \exp(-\mu v^2/2kT) dv, \quad (12)$$

where v is the relative velocity in the initial state, μ is the

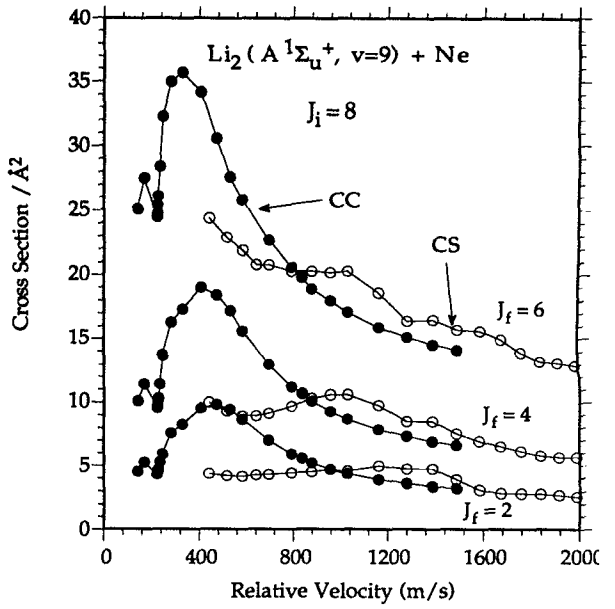

FIG. 11. Rotationally inelastic cross sections, as a function of the collision velocity, for downward ($J_{final} < J_{initial}$) transitions out of the $J = 8$ rotational level of the $v = 9$ manifold of $Li_2(A\ ^1\Sigma_u^+)$ in collisions with Ne. The filled circles denote the results of the present CC calculations while the open circles indicate the results of calculations done within the coupled-states (CS) approximation.

collision reduced mass, $\sigma(v)$ is the velocity-dependent cross section, and $N(T)$ is the usual normalization factor for a Maxwellian velocity distribution at temperature T. At the translational temperature of the experiments (705 K = 490 cm^{-1}),[5] the range of velocities effectively sampled extends beyond the highest velocity at which the CC scattering calculations were performed (1 580 cm^{-1} for $J = 8$). As a result, in order to evaluate the integral in Eq. (12) numerically, it is necessary to extrapolate the calculated cross sections to higher velocity. From Figs. 5–8 we see that the cross sections all rise to a maximum and then monotonically decrease as a function of collision velocity. Thus, for all transitions in which the cross sections have reached their maximum at the highest total energy used (900 cm^{-1} in the CC calculations and 1700 cm^{-1} in the CS calculations), we felt that it would be reasonable to extrapolate the cross sections to higher velocity using a simple power law function, $\sigma(v) = Av^{-\gamma}$.

Based on this extrapolation, thermal rate constants were computed from the calculated cross sections, and are compared with the experimental values in Fig. 12 for $J_{initial} = 8$ and, in Fig. 13, for $J_{initial} = 22$. We observe that the agreement between the calculated CC rate constants and the experimental values, at least for all the $J \rightarrow J'$ transitions for which the high-velocity power-law extrapolation could be used, is truly excellent, almost within the small reported experimental error limits. The reader should note that the experimental values have not been scaled prior to making the comparison shown in Figs. 12 and 13. We also observe that

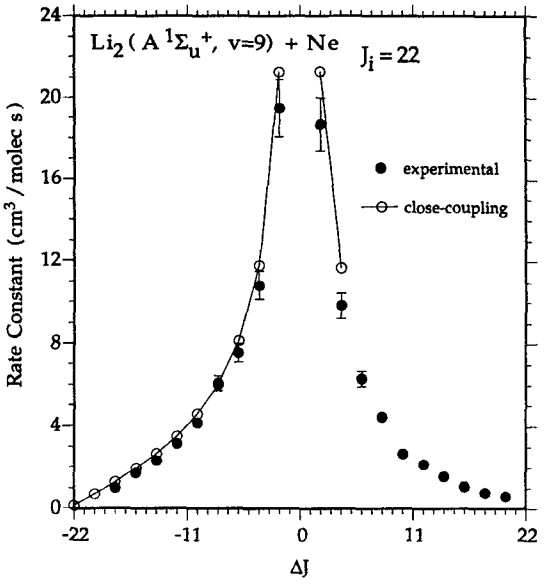

FIG. 13. Thermal rate constants at $T = 705$ K for rotationally inelastic transitions out of the $J = 22$ level of the $v = 9$ manifold of $Li_2(A\ ^1\Sigma_u^+)$ in collisions with Ne plotted as a function of the change in rotational quantum number. Filled circles: experimental values from Ref. 5; open circles: close coupled calculations. The calculated rate constants are displayed only up to the highest final state rotational quantum for which the $J \rightarrow J'$ cross sections had peaked at the highest total energy used in the calculations (900 cm^{-1} for CC) so that a power-law extrapolation could be used safely at high velocity.

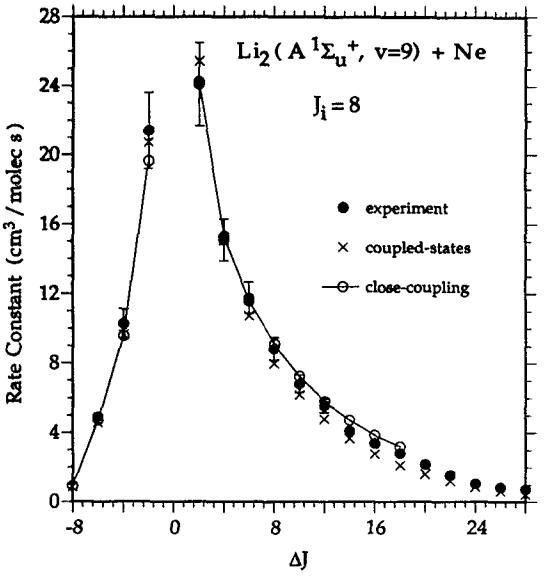

FIG. 12. Thermal rate constants at $T = 705$ K for rotationally inelastic transitions out of the $J = 8$ level of the $v = 9$ manifold of $Li_2(A\ ^1\Sigma_u^+)$ in collisions with Ne plotted as a function of the change in rotational quantum number. Filled circles: experimental values from Ref. 5; open circles: close coupled calculations; crosses: coupled states calculations. The calculated rate constants are displayed only up to the highest final state rotational quantum for which the $J \rightarrow J'$ cross sections had peaked at the highest total energy used in the calculations (900 cm^{-1} for CC and 1700 cm^{-1} for CS) so that a power-law extrapolation could be used safely at high velocity.

the considerable difference between the CC and CS cross sections seen in Figs. 10 and 11 is reduced substantially by the velocity averaging inherent in the thermal rate constants. [A similar effect of the velocity averaging could also underlie the good agreement[52,53] between the CC and CS rate constants for collisions of $OH(A\ ^2\Sigma^+)$ with Ar and He noted in Sec. VI.]

VIII. CONCLUSION

We have presented the results of full close-coupled calculations of rotationally inelastic cross sections for collisions of Li_2 in the $A\ ^1\Sigma_u^+$ electronic state with Ne, based on an accurate new *ab initio* potential energy surface. The magnitudes and the dependence on relative collision velocity of our calculated cross sections were seen to be in remarkably good agreement with the experimentally obtained values of Smith, Scott, and Pritchard.[4] Further, velocity averaged thermal rate constants determined from the calculated cross sections are in equally good agreement with the experimental values reported by these authors.[5]

The quality of the agreement confirms the accuracy of the *ab initio* points and the method used to fit these points. Alternatively, the good agreement can be seen as a confirmation of the accuracy of the experiment[4,5] and the subsequent analysis. Some disagreement with experiment does appear at lower collision velocities, where the variation in the calculated cross sections as either energetic or dynamical thresholds are approached is more pronounced than that seen experi-

mentally. This is likely a result of the considerable averaging associated with the doppler deconvolution method used.[4,15,16] Part of the error could also be due to inaccuracies of the long-range part of our *ab initio* potential. Hopefully the present theoretical calculations will act to stimulate further development of these or other[8,9] Doppler techniques, with the goal of an improved determination of inelastic cross sections near threshold.

The excellent agreement with experiment seen here, as well as in related earlier work on collisions of $OH(A\ ^2\Pi)$ with Ar (Ref. 53) and He,[52] indicate clearly that one can now determine atom–diatom *ab initio* potential energy surfaces to an accuracy sufficient to describe precisely rotationally, rovibrationally, and, even, electronic–rovibrationally[24,62,63] inelastic collision processes.

The degree of agreement between the velocity dependence of the full close-coupled cross sections and those obtained within the coupled-states approximation was discouraging. This may cast some doubt on the accuracy of the previous semiclassical coupled-states treatment of rotationally inelastic collisions of $Li_2(A)$ with Ne reported by Nyeland and Billing.[19] By contrast the CS approximation was seen to be considerably more accurate in the prediction of thermal rate constants, as a result of the substantial averaging over velocity which is inherent in these quantities.

In other work,[24] we have used the PES presented here to determine, within the CS approximation, cross sections for rovibrationally inelastic collisions of $Li_2(A\ ^1\Sigma_u^+)$ with Ne. Similar calculations, based on a model PES, have been reported by Maricq.[23] Of particular interest are the dramatic near resonant effects seen experimentally by Magill *et al.*[21,25] and explored theoretically by Magill,[21] Parson,[22] Maricq,[23] and their co-workers. The results of our preliminary CS calculations,[24] reproduce qualitatively these near resonant effects. Unfortunately, the relatively poor accuracy of the CS approximation for rotationally inelastic processes, seen in the present paper, may imply that for a meaningful comparison with experiment it may well be necessary to use full close coupling for an accurate determination of these rovibrationally inelastic cross sections, despite the enormity of the computational task.

ACKNOWLEDGMENTS

M.H.A. wishes to thank the Alexander von Humboldt Foundation for a Senior US Scientist award, during the tenure of which part of the work described here was carried out at the Universität Bielefeld, Germany. He would also like to thank the US National Science Foundation, under Grant No. CHE-8917543, for partial support of the work described herein. The participation of H.J.W. was made possible by the Deutsche Forschungsgemeinschaft (SFB 216) and by the German Fonds der Chemischen Industrie. The authors are grateful to Andre Zilch for his help with the *ab initio* calculations reported here and to Brian Stewart for helpful clarification concerning details of the experimental work reported in Ref. 5. The calculations were performed on the CRAY-YMP 8/32 of the Höchstleistungsrechenzentrum Jülich and at the Center for Intensive Computation at the University of Maryland, supported in part by a grant to M.H.A. by the U. S. Army Research Office under the DoD University Research Instrumentation program, Grant No. DAAG29-85-K-0018.

[1] K. Bergmann and W. Demtröder, Z. Physik **243**, 1 (1971).
[2] T. A. Brunner, R. D. Driver, N. Smith, and D. E. Pritchard, J. Chem. Phys. **70**, 4155 (1979).
[3] T. A. Brunner, N. Smith, A. Karp, and D. E. Pritchard, J. Chem. Phys. **74**, 3324 (1981).
[4] N. Smith, T. P. Scott, and D. E. Pritchard, J. Chem. Phys. **81**, 1229 (1984).
[5] T. P. Scott, N. Smith, and D. E. Pritchard, J. Chem. Phys. **80**, 4841 (1984).
[6] M. D. Rowe and A. J. McCaffery, Chem. Phys. **43**, 35 (1979).
[7] S. R. Jeyes, A. J. McCaffery, and M. D. Rowe, Mol. Phys. **36**, 1865 (1978).
[8] C. P. Fell, A. J. McCaffery, K. L. Reid, A. Ticktin, and B. J. Whitaker, Laser Chem. **9**, 219 (1988).
[9] A. J. McCaffery, M. J. Proctor, E. A. Seddon, and A. Ticktin, Chem. Phys. Lett. **132**, 181 (1986).
[10] J. Derouard, T. D. Nguyen, H. Debontride, and N. Sadeghi, J. Chem. Phys. **90**, 5936 (1989).
[11] J. Derouard, Chem. Phys. **84**, 181 (1984).
[12] T. A. Brunner, R. D. Driver, N. Smith, and D. E. Pritchard, Phys. Rev. Lett. **41**, 856 (1978).
[13] R. Ramaswamy, A. E. DePristo, and H. Rabitz, Chem. Phys. Lett. **61**, 495 (1979).
[14] N. Smith, T. A. Brunner, R. D. Driver, and D. E. Pritchard, J. Chem. Phys. **69**, 1498 (1978).
[15] J. Apt and D. E. Pritchard, Phys. Rev. Lett. **37**, 91 (1976).
[16] J. L. Kinsey, J. Chem. Phys. **66**, 2560 (1977).
[17] D. Lemoine, G. C. Corey, M. H. Alexander, and J. Derouard, Chem. Phys. **118**, 357 (1987).
[18] D. Poppe, Chem. Phys. Lett. **19**, 63 (1973).
[19] C. Nyeland and G. D. Billing, Chem. Phys. **138**, 245 (1989).
[20] L. K. Cooper, A. J. McCaffery, and S. D. Bosanac, Chem. Phys. Lett. **167**, 233 (1990).
[21] B. Stewart, P. D. Magill, T. P. Scott, J. Derouard, and D. E. Pritchard, Phys. Rev. Lett. **60**, 282 (1988); P. D. Magill, B. Stewart, N. Smith, and D. E. Pritchard, *ibid.* **60**, 1943 (1988).
[22] W. J. Hoving and R. Parson, Chem. Phys. Lett. **158**, 222 (1989).
[23] M. M. Maricq, Phys. Rev. A. **39**, 3710 (1989).
[24] M. H. Alexander, A. Berning, A. Degli-Esposti, A. Jörg, A. Kliesch, and H.-J. Werner, Ber. Bunsenges. Phys. Chem. **94**, 1253 (1990).
[25] P. D. Magill, T. P. Scott, N. Smith, and D. E. Pritchard, J. Chem. Phys. **90**, 7195 (1990).
[26] A. Arthurs and A. Dalgarno, Proc. R. Soc. London, Ser. A **256**, 540 (1960).
[27] D. J. Kouri, in *Atom–Molecule Collision Theory: A Guide for the Experimentalist*, edited by R. B. Berstein (Plenum, New York, 1979), p. 301.
[28] P. McGuire and D. J. Kouri, J. Chem. Phys. **60**, 2488 (1974).
[29] MOLPRO is a package of *ab initio* programs written by H.-J. Werner and P. J. Knowles, with contributions from J. Almlöf, R. Amos, S. Elbert, W. Meyer, E. A. Reinsch, R. Pitzer, and A. Stone.
[30] W. Müller and W. Meyer, J. Chem. Phys. **85**, 953 (1986).
[31] H.-J. Werner and W. Meyer, Phys. Rev. A **13**, 13 (1976).
[32] K. P. Huber and G. Herzberg, *Molecular Spectra and Molecular Structure. IV. Constants of Diatomic Molecules* (Van Nostrand Reinhold, New York, 1979).
[33] W. Müller and W. Meyer, J. Chem. Phys. **80**, 3311 (1984).
[34] I. Schmidt-Mink, W. Müller, and W. Meyer, Chem. Phys. **92**, 263 (1985).
[35] H.-J. Werner and P. J. Knowles, J. Chem. Phys. **82**, 5053 (1985).
[36] P. J. Knowles and H.-J. Werner, Chem. Phys. Lett. **115**, 259 (1985).
[37] H.-J. Werner, Adv. Chem. Phys. **49**, 1 (1987), and references contained therein.
[38] H.-J. Werner and P. J. Knowles, J. Chem. Phys. **89**, 5803 (1988).
[39] P. K. Knowles and H.-J. Werner, Chem. Phys. Lett. **145**, 514 (1988).
[40] S. F. Boys and F. Benardi, Mol. Phys. **19**, 553 (1970).
[41] R. Schinke, W. Müller, W. Meyer, and P. McGuire, J. Chem. Phys. **74**, 3916 (1981).
[42] K. Lee and J. M. Bowman, J. Chem. Phys. **85**, 6225 (1986).
[43] J. M. Hutson and B. J. Howard, Mol. Phys. **43**, 493 (1981).
[44] P. Kuprenie, E. A. Mason, and J. T. Vanderslice, J. Chem. Phys. **39**, 2399 (1963).

[45] A FORTRAN program to compute the Legendre expansion coefficients in Eqs. (10) and (11) is available on request from M.H.A. by electronic mail (address: mha@hibridon.umd.edu). Please supply a return electronic mail address.
[46] P. L. Jones, U. Hefter, A. Mattheus, J. Witt, K. Bergmann, W. Müller, W. Meyer, and R. Schinke, Phys. Rev. A (1982).
[47] F. H. Mies, J. Chem. Phys. **42**, 2709 (1965).
[48] W. A. Lester, Jr., Meth. Comp. Phys. **10**, 211 (1971).
[49] See, for example, D. Secrest, in *Atom–Molecule Collision Theory: A Guide for the Experimentalist,* edited by R. B. Bernstein (Plenum, New York, 1979), p. 265.
[50] H. Rabitz, J. Chem. Phys **63**, 5208 (1975).
[51] R. G. Gordon, Meth. Comput. Phys. **10**, 81 (1971).
[52] A. Jörg, A. Degli-Esposti, and H.-J. Werner, J. Chem. Phys. **93**, 8757 (1990).
[53] A. Degli-Esposti and H.-J. Werner, J. Chem. Phys. **93**, 3351 (1990).
[54] P. McGuire, Chem. Phys. **13**, 81 (1976).
[55] HIBRIDON is a package of programs for the time-independent quantum treatment of inelastic collisions and photodissociation written by M. H. Alexander, D. E. Manolopoulos, H.-J. Werner, and B. Follmeg, with contributions by P. F. Vohralik, D. Lemoine, G. Corey, B. Johnson, T. Orlikowski, W. Kearney, A. Berning, and A. Degli-Esposti.
[56] See AIP document no. PAPS JCPSA-95-6524-6 for 6 pages of numerical values of the cross sections displayed in Figs. 5–8. Order by PAPS number and journal references from American Institute of Physics, Physics Auxiliary Publication Service, 335 East 45th Street, New York, NY 10017. The price is $1.50 for each microfiche (98 pages) or $5.00 for photocopies of up to 30 pages, and $0.15 for each additional page over 30 pages. Airmail additional. Make checks payable to the American Institute of Physics.
[57] W. H. Miller, J. Chem. Phys. **53**, 3578 (1970).
[58] S. Green, Chem. Phys. Lett. **38**, 293 (1976).
[59] L. N. Smith and D. Secrest, J. Chem. Phys. **74**, 3882 (1981).
[60] S. Green, J. Chem. Phys. XX, yyyy (1991).
[61] K. J. Laidler, *Theories of Chemical Reaction Rates* (McGraw-Hill, New York, 1969).
[62] H.-J. Werner, B. Follmeg, and M. H. Alexander, J. Chem. Phys. **89**, 3139 (1988).
[63] H.-J. Werner, B. Follmeg, M. H. Alexander, and D. Lemoine, J. Chem. Phys. **91**, 5425 (1989).